



## Fc-engineered monoclonal antibodies to reduce off-target liver uptake

Tristan Mangeat, Matthieu Gracia, Alexandre Pichard, Sophie Poty, Pierre Martineau, Bruno Robert, Emmanuel Deshayes

### ► To cite this version:

Tristan Mangeat, Matthieu Gracia, Alexandre Pichard, Sophie Poty, Pierre Martineau, et al.. Fc-engineered monoclonal antibodies to reduce off-target liver uptake. *EJNMMI Research*, 2023, 13 (1), pp.81. 10.1186/s13550-023-01030-0 . hal-04598633

**HAL Id: hal-04598633**

**<https://hal.science/hal-04598633>**

Submitted on 3 Jun 2024

**HAL** is a multi-disciplinary open access archive for the deposit and dissemination of scientific research documents, whether they are published or not. The documents may come from teaching and research institutions in France or abroad, or from public or private research centers.

L'archive ouverte pluridisciplinaire **HAL**, est destinée au dépôt et à la diffusion de documents scientifiques de niveau recherche, publiés ou non, émanant des établissements d'enseignement et de recherche français ou étrangers, des laboratoires publics ou privés.




Distributed under a Creative Commons Attribution 4.0 International License

PRELIMINARY RESEARCH

Open Access



# Fc-engineered monoclonal antibodies to reduce off-target liver uptake

Tristan Mangeat<sup>1†</sup>, Matthieu Gracia<sup>1†</sup>, Alexandre Pichard<sup>1</sup>, Sophie Poty<sup>1</sup>, Pierre Martineau<sup>1</sup>, Bruno Robert<sup>1,3\*†</sup> and Emmanuel Deshayes<sup>1,2,3\*†</sup> 

## Abstract

**Background** Radiolabeled-antibodies usually display non-specific liver accumulation that may impair image analysis and antibody biodistribution. Here, we investigated whether Fc silencing influenced antibody biodistribution. We compared recombinant <sup>89</sup>Zr-labeled antibodies (human IgG1 against different targets) with wild-type Fc and with mutated Fc (LALAPG triple mutation to prevent binding to Fc gamma receptors; FcγR). After antibody injection in mice harboring xenografts of different tumor cell lines or of immortalized human myoblasts, we analyzed antibody biodistribution by PET-CT and conventional biodistribution analysis.

**Results** Accumulation in liver was strongly reduced and tumor-specific targeting was increased for the antibodies with mutated Fc compared with wild-type Fc.

**Conclusion** Antibodies with reduced binding to FcγR display lower liver accumulation and better tumor-to-liver ratios. These findings need to be taken into account to improve antibody-based theragnostic approaches.

**Keywords** PET-CT, Fc gamma receptor, Off-target, Fc, LALAPG mutation

## Introduction

Off-target binding of drugs is a common problem in diagnostic and therapeutic settings. This is also the case for antibodies, although unlike other drugs, they bind to a specific target mainly due to the exquisite specificity of their antigen-binding fragment. In oncology, this sought-after high specificity can induce off-tumour binding because, to date, most antibody targets are

over-expressed in tumour tissue (on-target, on-tumour), but they can also be expressed at basal levels in healthy tissue (on-target, off-tumour). In addition, the crystallizable (Fc) region of the antibody fragment can also induce off-target binding by interacting with Fc gamma receptors (FcγR), which are expressed in many tissues, in particular by liver Kupffer cells in addition to being expressed on the surface of cells of the immune system. To counteract this, certain antibodies are now selected with a lower specific affinity to reduce their off-target binding [1] or by re-engineering [2]. Concerning the Fc domain, mutations N297-A or -D, L234A/L235A (LALA), G236R/L328R (RR), S298G/T299A (GA) and S228P/L235E (IgG4-PE) significantly reduce binding to Fc gamma receptors (FcγRI and FcγRIIA) [3–5], and the triple mutation L234A/L235A/P329G (LALAPG) significantly reduces binding to all FcγRs [5]. Several studies have shown that the introduction of the N297A or S228/L235E mutations has no impact on the tumour localization of several antibodies but does allow a longer half-life for antibodies carrying these mutations via reduced

<sup>†</sup>Tristan Mangeat, Matthieu Gracia, Bruno Robert and Emmanuel Deshayes have contributed equally to this work.

\*Correspondence:

Bruno Robert

bruno.robert@inserm.fr

Emmanuel Deshayes

emmanuel.deshayes@icm.unicancer.fr

<sup>1</sup> Institut de Recherche en Cancérologie de Montpellier (IRCM), Inserm U1194, Université de Montpellier, ICM, 34298 Montpellier, France

<sup>2</sup> Institut Régional du Cancer de Montpellier (ICM), Service de Médecine Nucléaire, 34298 Montpellier, France

<sup>3</sup> Institut de Recherche en Cancérologie de Montpellier (IRCM), 124 Avenue des Apothicaires, 34090 Montpellier, France

catabolism by the liver [6–8]. In this study, we compared the biodistribution of  $^{89}\text{Zr}$ -labelled antibodies carrying the LALAPG triple mutation (Fc-LALAPG) with the same antibodies carrying a wild-type Fc, as these triple mutations are even more potent than N297D mutation in abolishing Fc $\gamma$ R binding and some clinical trials using mAbs incorporating these triple mutations are in progress [5].

## Materials and methods

### Recombinant antibody production

D4a mAb (patent number WO2016091891A1) is specific to human AXL tyrosine kinase receptor since it does not bind to mouse Axl and other human receptors of the same family, TYRO3 or MER tyrosine kinase receptors. 13R4a mAb is specific of *E. coli* beta-galactosidase specific and this antibody is used as an isotype irrelevant control [9]. Interestingly, the synthetic library is build using 13R4a clone as template, meaning that there are only few differences between D4a and 13R4a exclusively located in the 6 CDR loops. These two mAbs have been isolated in the laboratory from a human synthetic library of scFv using phage display [10]. ScFv were reformatted as full human IgG1 with wild type (WT) Fc by cloning variable heavy and light chain in an expression plasmid. The L234A/L235A/P329G mutations were introduced in coding plasmid by targeted PCR-mutagenesis and validated by sequencing. 13R4a and D4a antibodies with wild type Fc and with the L234A/L235A/P329G mutation (LALAPG Fc) were produced in HEK293T cells by transient transfection with polyethylenimine. Antibodies were purified from supernatant using Protein-A agarose beads and dialyzed against PBS. Purity was verified on SDS-PAGE. Antibody binding was validated in vitro by enzyme linked immunosorbent assay and by fluorescent-activated cell sorting in different cell lines.

### Radioimmunoconjugation

Antibodies (human IgG format) were functionalized with pSCN-Bn-deferoxamine in a non-site-specific manner before radiolabeling with  $^{89}\text{Zr}$ . Briefly, the antibody buffer was exchanged to chelexed PBS using Amicon® Ultra Centrifugal filters (30 kDa cut-off). pH was adjusted to 8.5–9.0 using 0.2 M chelexed  $\text{Na}_2\text{CO}_3$ , and a 15-fold excess of pSCN-Bn-deferoxamine was added to the solution (1.6–2.1 mg/mL, 500  $\mu\text{L}$ ). After incubation at 37 °C with gentle shaking for 60 min, excess pSCN-Bn-deferoxamine was removed using Amicon® Ultra Centrifugal filters as before.  $^{89}\text{Zr}$  Zr-oxalate (Perkin Elmer) (30 MBq) was neutralized to pH 6.9–7.2 with 1 M chelexed  $\text{Na}_2\text{CO}_3$  before addition of the deferoxamine-immunoconjugates

and incubation at room temperature with gentle shaking for 1 h. Purity and radiolabeling efficiencies were determined using instant thin-layer chromatography with 0.1 M sodium citrate (pH 5.0) as mobile phase. Radiolabeling yield and radiochemical purity were routinely > 99%. No purification step was performed. Radioimmunoconjugates had a specific activity of 200 MBq/mg and were formulated in 0.9% NaCl for in vivo use. Analysis of the immunoconjugate was performed by Maldi-tof (Rapiflex, Bruker) to determine the number of DFO conjugated to mAbs. The number of DFO molecules is determined by dividing the difference in the m/s ratio of the peak of the whole antibody conjugated with DFO and unconjugated with the molecular weight of DFO (752 Da) (Additional file 1: Figure S1). Binding affinity of D4a mAbs conjugated with DFO was performed by flow cytometry using AXL expressing cell line. A binding affinity experiment was presented in Additional file 1: Figure S2.

### Cell lines and mice

The AXL-expressing [11, 12] human MDA-MB-231 (triple negative breast cancer) and CFPAC-1 (pancreatic cancer) cell lines were from American Type Culture Collection. Immortalized human myoblasts (provided by Vincent Mouly, UMR-S 974) express low AXL level and were used to mimic healthy human tissues. Cancer cells were cultured in Dulbecco's Modified Eagle's Medium (DMEM) with 10% Fetal Bovine Serum (FBS, Eurobio), and myoblasts in skeletal muscle cell growth medium (C-23060, Promocell) with 20% FBS at 37 °C and 5%  $\text{CO}_2$ . All animal experiments were performed in compliance with the European directive (2010/63/EU) and the INSERM standards for experimental animal studies (agreement E34-172-27). They were approved by the Institut de Recherche en Cancérologie de Montpellier region (IRCM/INSERM U1194) and the Languedoc Roussillon region (CEEALR France No. 36) ethics committees. Cells ( $5 \times 10^6$ ) in Matrigel (Corning) were injected subcutaneously in 6-week-old female athymic nude mice (CrI: Nu (NCR)-Foxn1nu, Charles River).

### Imaging

Four weeks after cell xenografts,  $^{89}\text{Zr}$  Zr-deferoxamine-labeled antibodies (50  $\mu\text{g}$ , 200 MBq/mg) were injected in the tail vein and in vivo images were acquired with a Mediso NanoScan PET82S/CT80 system at 48, 72, and 96 h post-injection. Anesthesia was induced with 4% isoflurane in air followed by maintenance with 2% isoflurane in air. Images were acquired with Nuclide and processed

with Interview™ Fusion™. Volumes of interests were manually drawn on fused PET-CT images using 3D Slicer. Results are expressed as percentage of the injected activity per  $\text{cm}^3$  ( $\%IA/\text{cm}^3$ ).

### Conventional biodistribution analysis

Biodistribution was assessed at 96 h post-injection after the last imaging time-point. After euthanasia, tumor, myoblast xenografts, and liver were excised, weighted, and activity counted with a gamma-counter (Hidex AMG) together with standards of the injected radiolabeled antibodies. Results were expressed as percentage of the injected activity per gram of tissue ( $\%IA/g$ ).

## Results

### Imaging

First, we studied the biodistribution of the 13R4a IgG against bacterial  $\beta$ -galactosidase that is not expressed in mice to avoid the effect of the targeted antigen. To respect the 3R rules, we used mice previously xenografted with immortalized myoblasts (left flank). At 48, 72 and 96 h after injection of  $^{89}\text{Zr}$ -radiolabeled 13R4a

antibodies with wild-type Fc or LALAPG Fc, PET images showed a strong accumulation of 13R4a with wild-type Fc in liver (Fig. 1A, up) and a weak accumulation of 13R4a with LALAPG Fc (Fig. 1A, down). We observed accumulation in joints (shoulder and knee) particularly of the wild-type antibody, possibly explained by the natural tropism of zirconium 89 for bones and joints [13]. Quantification of liver uptake confirmed a decrease in liver accumulation by threefold at 48 h ( $5.4$  vs  $16.2\%IA/\text{cm}^3$ ) and by twofold at 96 h ( $5.1$  vs  $13.1\%IA/\text{cm}^3$ ) of 13R4a-LALAPG Fc compared with 13R4a-wild-type Fc (Fig. 1B). As 13R4a does not recognize any target in mice, we then used D4a, an antibody against human (but not mouse) AXL, and three human cell lines with different AXL expression: immortalized myoblasts (low AXL expression) and MDA-MB-231 and CFPAC cancer cells (high AXL expression). We injected  $^{89}\text{Zr}$ -radiolabeled D4a with wild-type Fc in mice xenografted with myoblasts (left flank) and with CFPAC-1 cells (right flank) and  $^{89}\text{Zr}$ -radiolabeled D4a with LALAPG Fc in mice xenografted with myoblasts (left flank) and MDA-MB-231 cells (right flank). We could not quantify antibody accumulation in

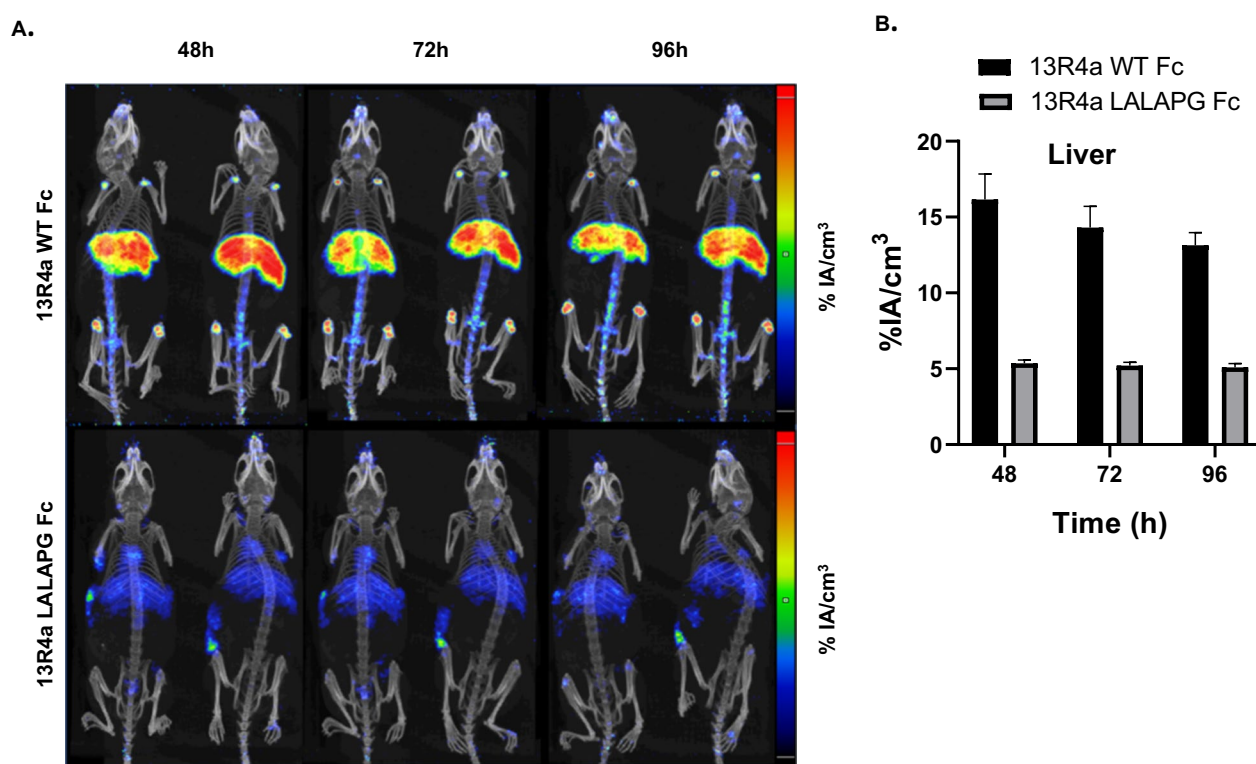


**Fig. 1** Liver accumulation of a bacterial anti-beta galactosidase IgG is reduced by the LALAPG triple mutation. **A** Maximal Intensity Projection (MIP) PET images of mice subcutaneously xenografted with myoblasts (left flank) at 48, 72 and 96 h after the injection of  $^{89}\text{Zr}$ -radioimmunolabeled 13R4a with LALAPG Fc or with WT Fc ( $n=2$  mice per group). The low and high values correspond to 1 and 5%  $IA/\text{cm}^3$  respectively and are indicated by a low and high line on the scale. **B** Quantitative PET analysis (PET based) of antibody accumulation in liver at different times post-injection (48 h, 72 h and 96 h) expressed in  $\%IA/\text{cm}^3$



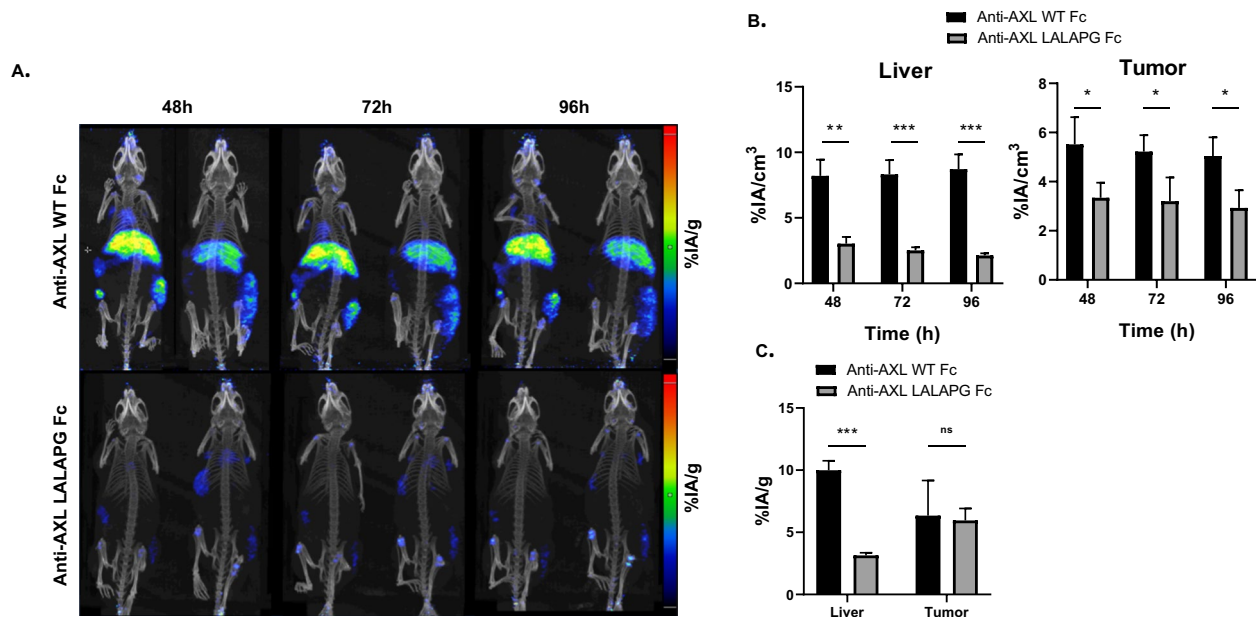


**Fig. 2** Anti-AXL D4a IgG with LALAPG Fc displays lower liver retention than the IgG with WT Fc. **A** Maximal Intensity Projection PET images of mice subcutaneously xenografted with myoblasts (left flank) and tumor cells (right flank; CFPAC-1 cells for the IgG with WT Fc and MDA-MB-231 cells for the IgG with LALAPG Fc) at 48, 72 and 96 h after injection of <sup>89</sup>Zr-radioimmuno-labeled anti-AXL D4a IgG with LALAPG Fc or WT Fc ( $n=3$  mice per group). The low and high values correspond to 1 and 5% AI/g respectively and are indicated by a low and high line on the scale. **B** Quantitative PET analysis of anti-AXL IgG in liver at 48 h, 72 h and 96 h post-injection, expressed in %IA/cm<sup>3</sup>. **C** Conventional biodistribution analysis of the anti-AXL IgG in liver and tumors (CFPAC-1 cells for the IgG with WT Fc and MDA-MB-231 cells for the IgG with LALAPG Fc) at 96 h post-injection. The percentage of activity in the organ (%IA/g) corresponds to the injected activity related to the organ weight. For panels **B** and **C**:  $*p \leq 0.05$ ,  $**p \leq 0.01$ ,  $***p \leq 0.001$ ; ns, not significant (unpaired two-tailed  $t$  test)

myoblast xenografts due to spatial resolution and xenograft size limitations. Like with 13R4a, D4a with wild-type Fc strongly accumulated in liver at 48, 72 and 96 h post injection (Fig. 2A, up), but not D4a with LALAPG Fc (Fig. 2A, down). Quantification at 96 h confirmed the significantly lower liver retention of D4a with LALAPG Fc than with wild-type Fc ( $2.1 \pm 0.2$  vs  $8.7 \pm 1.1$  %IA/cm<sup>3</sup>;  $p < 0.001$ ) (Fig. 2B). Our findings demonstrate that the LALAPG mutation in the Fc region reduced drastically the liver retention of two antibodies (D4a and 13R4a).

#### Biodistribution analysis

The biodistribution study showed a reduced (by four-fold) liver accumulation of <sup>89</sup>Zr-radiolabeled D4a with LALAPG Fc compared with wild-type Fc at 96 h ( $3.1 \pm 0.2$  vs  $10.0 \pm 0.8$  %IA/g;  $p < 0.001$ ) (Fig. 2C). Accumulation in CFPAC-1 and MDA-MB-231 tumors was modest for both D4a with wild type and with LALAPG Fc ( $6.3 \pm 2.8$  and  $6.0 \pm 1.0$  %IA/g). However, the tumor-to-liver ratio for D4a with LALAPG Fc was 1.9 (vs 0.6) thanks to the very low liver accumulation.

#### Discussion

We demonstrated that the LALAPG triple mutation in the Fc region strongly reduces accumulation in liver of <sup>89</sup>Zr-radiolabeled antibodies. Liver accumulation of metal-radiolabeled antibodies is frequently observed in diagnostic and therapeutic settings [14, 15]. A previous biodistribution study showed that an afucosylated IgG promotes higher liver accumulation mediated by FcγR binding [7]. Reducing this binding, without affecting the antibody half-life, could decrease liver accumulation. Therefore, we used antibodies harboring a triple Fc mutation (LALAPG) that negatively affects binding to all murine FcγR [16]. Dekkers et al. demonstrated a similar binding profile of human IgG1 and mouse IgG2a to mouse FcγR [17]. The very low liver accumulation of human IgG1 with LALAPG Fc in our study can be explained by reduced interactions with mouse FcγR on hepatocytes and resident macrophages [6, 18]. This lower liver accumulation should allow antibody redistribution and favor their accumulation in tissues/tumors that express the targeted antigen. Another study showed

that the N297A mutation in the Fc region of avelumab hampers FcγR binding and improves its plasma half-life in monkeys [19]. Moreover, deglycosylation (to impair FcγRI binding) of an immunoconjugate reduced the off-target uptake and increased the tumor uptake [8].

The LALAPG Fc mutation could be used to optimize therapy or diagnosis by reducing liver off-target uptake. For imaging purposes, decreasing the unspecific liver uptake is especially valuable to reinforce the contrast of liver tumors/metastases. With therapeutic (alpha, beta particles) emitters, reducing liver off-target accumulation would diminish unspecific liver irradiation. We need now to confirm the hypothesis that reducing off-target liver accumulation improves the antibody biodistribution, resulting in higher tumor uptake.

## Conclusion

We reduced non-specific liver accumulation by using antibodies harboring the LALAPG mutation in the Fc region. This could be a strategy to optimize the targeting specificity of radioimmunoconjugates used for diagnostic and therapeutic purposes.

## Abbreviations

<sup>89</sup> Zr	Zirconium 89
DMEM	Dulbecco's Modified Eagle's Medium
FBS	Fetal Bovine Serum
Fc	Fragment crystallizable
FcγR	Fc gamma receptors
IgG	Immunoglobulin G
PBS	Phosphate buffered saline
PEI	Polyethylenimine
PET-CT	Positron emission tomography-computed tomography
WT	Wild type

## Supplementary Information

The online version contains supplementary material available at <https://doi.org/10.1186/s13550-023-01030-0>.

**Additional file 1. Figure S1:** Example of mass-analysis of mAbs conjugated with DFO. Analysis of the immunoconjugate was performed by MALDI-toF (Rapiflex, Bruker) to determine the number of DFO conjugated to mAbs. Peaks of the entire antibody are indicated by an arrow. **Figure S2:** Binding of D4a WT Fc and D4a LALAPG Fc after DFO conjugation on cancer cells by flow cytometry. Anti-AXL antibody D4a with WT Fc and with LALAPG mutations were used at 5 µg/ml to stain AXL positive cell line for 1 h at 4°C in PBS-BSA buffer. After 3 wash, a secondary fluorescent labeled anti-hFc mAbs labeled was used to reveal binding of D4a mAbs at the cell surface of the cell.

## Acknowledgements

We thank Yann Dromard, IRCM preclinical imaging platform, for support, Vincent Mouly, Myology center (UMR-S 974), for immortalized myoblasts, the IRCM PEFO platform for animal facilities, the BNIF platform for imaging facilities, and Diego Tosi for advice in the study design.

## Author contributions

TM and MG equally contributed to this work (in vitro, *in cellulo*, in vivo) and to writing manuscript. AP contributed to provide and analyzed PET-CT data. SP contributed to analyze PET-CT data. PM contributed to writing manuscript. BR and ED equally contributing to the supervision of this work. All authors read and approved the final manuscript.

## Funding

T. Mangeat had a PhD studentship from the Ligue Nationale Contre le Cancer. This work was supported by a grant of Ligue Régionale contre le Cancer de la Lozère; the French National Research Agency under the program Investissements d'Avenir Grant Agreement LabEx MABImprove (Grant No. ANR-10-LABX-53) and the Site de Recherche Intégrée sur le Cancer (SIRIC) Montpellier-Cancer (Grant No. INCa-DGOS-Inserm 6045).

## Availability of data and materials

The datasets used and/or analyzed during the current study are available from the corresponding author on reasonable request.

## Declarations

## Ethics approval and consent to participate

All animal experiments were performed in compliance with the European directive (2010/63/EU) and the INSERM standards for experimental animal studies (agreement E34-172-27). They were approved by the Institut de Recherche en Cancérologie de Montpellier (IRCM/INSERM U1194) and the Languedoc Roussillon region (CEEA LR France No. 36) ethics committees. A statement confirming the study was carried out in compliance with the ARRIVE guidelines.

## Consent for publication

Not applicable.

## Competing interests

Authors have no competing of interest to disclose.

Received: 17 May 2023 Accepted: 28 August 2023

Published online: 11 September 2023

## References

- Wong OK, Tran TT, Ho WH, et al. RN765C, a low affinity EGFR antibody drug conjugate with potent anti-tumor activity in preclinical solid tumor models. *Oncotarget*. 2018;9(71):33446.
- Slaga D, Ellerman D, Lombana TN, et al. Avidity-based binding to HER2 results in selective killing of HER2-overexpressing cells by anti-HER2/CD3. *Sci Transl Med*. 2018;10(463):5775.
- Sazinsky SL, Ott RG, Silver NW, Tidor B, Ravetch JV, Wittrup KD. Aglycosylated immunoglobulin G<sub>1</sub> variants productively engage activating Fc receptors. *Proc Natl Acad Sci USA*. 2008;105(51):20167–72.
- Liu R, Oldham R, Teal E, Beers S, Cragg M. Fc-engineering for modulated effector functions—improving antibodies for cancer treatment. *Antibodies*. 2020;9(4):64.
- Schlothauer T, Herter S, Koller CF, et al. Novel human IgG1 and IgG4 Fc-engineered antibodies with completely abolished immune effector functions. *Protein Eng Des Sel*. 2016;29(10):457–66.
- Sharma SK, Chow A, Monette S, et al. Fc-mediated anomalous biodistribution of therapeutic antibodies in immunodeficient mouse models. *Can Res*. 2018;78(7):1820–32.
- Sharma SK, Suzuki M, Xu H, et al. Influence of Fc modifications and IgG subclass on biodistribution of humanized antibodies targeting L1CAM. *J Nucl Med*. 2022;63(4):629–36.
- Vivier D, Sharma SK, Adumeau P, et al. The impact of FcγRI binding on immuno-PET. *J Nucl Med*. 2019;60(8):1174–82.
- Martineau P, Jones P, Winter G. Expression of an antibody fragment at high levels in the bacterial cytoplasm. *J Mol Biol*. 1998;280(1):117–27.
- Robin G, Sato Y, Desplancq D, et al. Restricted diversity of antigen binding residues of antibodies revealed by computational alanine scanning of 227 antibody-antigen complexes. *J Mol Biol*. 2014;426(22):3729–43.

11. Leconet W. Preclinical validation of AXL receptor as a target for antibody-based pancreatic cancer immunotherapy. *Oncogene*. 2014;33(47):5405–14.
12. Leconet W, Chentouf M, du Manoir S, et al. Therapeutic activity of anti-AXL antibody against triple-negative breast cancer patient-derived xenografts and metastasis. *Clin Cancer Res*. 2017;23(11):2806–16.
13. Chomet M, Schreurs M, Bolijn MJ, et al. Head-to-head comparison of DFO\* and DFO chelators: selection of the best candidate for clinical 89Zr-immuno-PET. *Eur J Nucl Med Mol Imaging*. 2021;48(3):694–707.
14. Boyle CC, Paine AJ, Mather SJ. The mechanism of hepatic uptake of a radiolabelled monoclonal antibody. *Int J Cancer*. 1992;50(6):912–7.
15. Hosseinimehr SJ, Tolmachev V, Orlova A. Liver uptake of radiolabeled targeting proteins and peptides: considerations for targeting peptide conjugate design. *Drug Discov Today*. 2012;17(21–22):1224–32.
16. Lo M, Kim HS, Tong RK, et al. Effector-attenuating substitutions that maintain antibody stability and reduce toxicity in mice. *J Biol Chem*. 2017;292(9):3900–8.
17. Dekkers G, Bentlage AEH, Stegmann TC, et al. Affinity of human IgG subclasses to mouse Fc gamma receptors. *MAbs*. 2017;9(5):767–73.
18. Bruggeman CW, Houtzager J, Dierdorp B, et al. Tissue-specific expression of IgG receptors by human macrophages ex vivo. *PLoS ONE*. 2019;14(10):e0223264.
19. Jin H, D'Urso V, Neuteboom B, McKenna SD, et al. Avelumab internalization by human circulating immune cells is mediated by both Fc gamma receptor and PD-L1 binding. *Oncol Immunology*. 2021;10:1958590.

## Publisher's Note

Springer Nature remains neutral with regard to jurisdictional claims in published maps and institutional affiliations.

**Submit your manuscript to a SpringerOpen<sup>®</sup> journal and benefit from:**

- Convenient online submission
- Rigorous peer review
- Open access: articles freely available online
- High visibility within the field
- Retaining the copyright to your article

---

Submit your next manuscript at ► [springeropen.com](https://www.springeropen.com)

---